

Electronic Supplementary Material (ESI)

**Quantifying the photocatalytic role and activity at the edge
and surface of Pd co-catalysts using N₂ fixation as a case**

Shijie Wu,^{‡a} Jiafei Zhang,^{‡a,b} Wenbin Chen,^a Pingxing Xing,^a Xingchen
Liu,^c Botao Teng,^{*a,b} Leihong Zhao,^{*a} and Song Bai^{*a}

^a Key Laboratory of the Ministry of Education for Advanced Catalysis Materials,
College of Chemistry and Life Sciences, Zhejiang Normal University, Jinhua, 321004,
China.

^b Tianjin Key Laboratory of Brine Chemical Engineering and Resource Eco-
utilization, College of Chemical Engineering and Materials Science, Tianjin
University of Science and Technology, Tianjin, 300457, China.

^c State Key Laboratory of Coal Conversion, Institute of Coal Chemistry, Chinese
Academy of Sciences, Taiyuan, 030001, China.

E-mail: tbt@zjnu.cn; zhaoleihong@163.com; songbai@zjnu.edu.cn

Additional experimental

Chemicals

K_2PdCl_4 (98%), Palladium chloride (PdCl_2), palladium (II) acetylacetonate ($\text{Pd}(\text{acac})_2$, 99%), iron (II) acetylacetonate ($\text{Fe}(\text{acac})_2$, 98%) were all purchased from Sigma-Aladdin. Poly(vinyl pyrrolidone) (PVP, M.W. \approx 55000 and M.W. \approx 8000) were all purchased from Aldrich. Polyallylamine hydrochloride (PAH, M.W. \approx 1,5000) was purchased from Energy Chemical. All other chemicals were of analytical grade and purchased from Sinopharm Chemical Reagent Co. Ltd. (Shanghai, China). All the chemicals were used as received without further purification. The water used in all experiments was deionized water prepared by passing through an ultra-pure purification system.

Synthesis of TiO_2 nanosheets

TiO_2 nanosheets were synthesized by modifying a method in the literature with hydrofluoric acid as a capping agent.^{S1} In a typical experimental procedure, 10 mL of tetrabutyl titanate ($\text{Ti}(\text{OBu})_4$) and 2.5 mL of hydrofluoric acid (HF) were mixed in a 50 mL Teflon-lined autoclave with under magnetic stirring. Then 0.5 mL trifluoroacetic acid (TFA) was dropped into the Teflon-lined stainless autoclave, which was heated at 200 °C for 24 h. After naturally cooling down to room temperature, the precipitate was collected by centrifuging the suspension, washed with water thoroughly, and then dried at 50 °C in a vacuum. Caution! HF is extremely corrosive and toxic, and should be handled with extreme care.

Catalyst characterizations

Transmission electron microscopy (TEM) and high-resolution TEM (HRTEM) images were taken on a JEOL JEM-2100F field-emission high-resolution transmission electron microscope operated at 200 kV. Powder X-ray powder diffraction (XRD) patterns were collected on a D8 Advance X-ray diffractometer with Non-monochromated $\text{Cu-K}\alpha$ X-Ray. X-ray photoelectron spectra (XPS) were

collected on an ESCALab 250 X-ray photoelectron spectrometer, using nonmonochromatized Al-K α X-ray as the excitation source. UV-vis-NIR diffuse reflectance data were recorded in the spectral region of 200-800 nm with a Shimadzu SolidSpec-3700 spectrophotometer. Photoluminescence (PL) spectra were recorded on a HITACHIF-7000 Spectrofluorometer with an excitation wavelength of 315 nm. The Brunauer-Emmett-Teller (BET) surface area and N₂ adsorption were tested using a Quantachrome autosorb iQ analyzer at 77 and 273 K, respectively. N₂-TPD profiles were recorded by a catalyst analyzer BELCAT II. ¹H-NMR spectra were obtained with a Bruker Avance 600WB nuclear magnetic resonance spectrometer (298 K, 600 MHz).

Photocatalytic N₂ fixation measurements

The photocatalytic activities of the synthesized TiO₂-Pd were evaluated by photocatalytic dinitrogen fixation under UV light. The photocatalytic N₂ fixation experiments were carried out in N₂ atmosphere at room temperature. Before UV light irradiation, 0.1 g of solid catalyst was added into a 200 mL ethanol solution (containing 10 mL ethanol and 190 mL water) and stirred for 1 h in the dark to ensure an adsorption-desorption equilibrium. UV light (320 < λ < 420 nm) was used as the illumination source, which was realized in the presence of a short-wave-pass 420 nm cutoff filter. The power density of UV light was measured to be 150 mW cm⁻². At every 1 h interval of irradiation, 6 mL of suspension was collected and centrifuged to obtain liquid samples. NH₄⁺ concentration analysis was conducted using Nessler's reagent method, at λ = 420 nm in a UV-vis spectrophotometer.

Photoelectrochemical measurements

4.0 mg of as-synthesized products were dispersed in a mixture of 10 μ L ethanol and 10 μ L Nafion, which were then uniformly spin-dropped onto at a 1 cm \times 1 cm indium tin oxide (ITO)-coated glass by a spin coater (SC-1B, China). Subsequently, the ITO-coated glasses were heated at 80 $^{\circ}$ C in a vacuum oven for 1 h. The photocurrents were measured on a CHI 760E electrochemical station (Shanghai

Chenhua, China) in ambient conditions under irradiation of a 300 W Xe lamp (PLS-SXE300/300UV, Beijing Perfectlight, China). UV light ($320 < \lambda < 420$ nm) was used as the illumination source, which was realized in the presence of a short-wave-pass 420 nm cutoff filter. The power density of UV light was measured to be 150 mW cm^{-2} . A three-electrode cell was used to perform the electrochemical measurements. The working electrode was the ITO-coated glass. An Ag/AgCl electrode and Pt foil were used as the reference electrode and counter electrode, respectively. The three electrodes were inserted in a quartz cell filled with Ar-saturated and N_2 -saturated $0.5 \text{ M Na}_2\text{SO}_4$ electrolyte, respectively. The photoresponse of the prepared photoelectrodes (i.e., I-t) was obtained by measuring the photocurrent density under chopped light irradiation (light on/off cycles: 60 s) at a bias potential of $0.4 \text{ V vs. Ag/AgCl}$ for 600 s.

TOF calculation methods

Since the surface area of TiO_2 and TiO_2 -Pd is similar, it is reasonably supposed that the difference of photocatalytic performance is due to the change of the sizes of Pd nanoparticles. Hence the activities of Pd cocatalysts were obtained by subtracting the value of TiO_2 ($46.5 \mu\text{mol g}_{\text{cat}}^{-1} \text{ h}^{-1}$), as shown in the following equation.

$$r_{Pd} = r_{\text{TiO}_2\text{-Pd}} - r_{\text{TiO}_2}$$

Then the TOF of Pd cocatalyst was calculated as: $TOF_{Pd} = r_{Pd}/N_{Pd}$

Where N_{Pd} is the number Pd atom at the edge and surface of Pd nanoparticle.

Since the activity of Pd cocatalyst is contributed by the edge and surface, the TOF on Pd nanoparticles with the same surface area and different edge-to-surface atomic ratio can be calculated as follows:

$$TOF_{Pd} = TOF_{Pd\text{-edge}} \times ratio_{Pd\text{-edge}} + TOF_{Pd\text{-surface}} \times ratio_{Pd\text{-surface}}$$

Where $TOF_{Pd\text{-edge}}$ and $TOF_{Pd\text{-surface}}$ are the turnover frequencies of Pd atom at the edge and surface, respectively, and their values should be larger than 0; $ratio_{Pd\text{-edge}}$ and $ratio_{Pd\text{-surface}}$ are the ratios of Pd atom at the edge and surface, respectively, and their values are listed in Table S1. Then $TOF_{Pd\text{-edge}}$ and $TOF_{Pd\text{-surface}}$ were calculated by

solving the equations above.

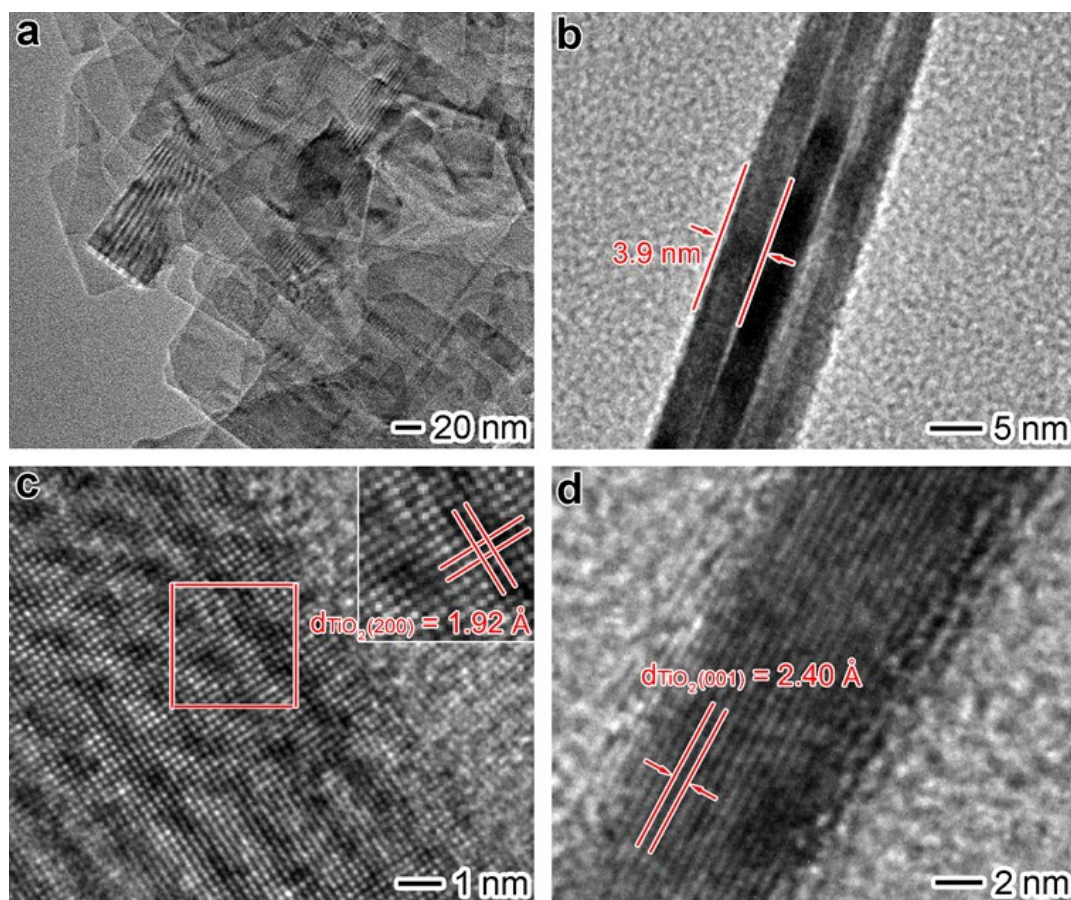


Fig. S1 TEM and HRTEM images of TiO₂ nanosheets: (a) TEM image showing the flat surface of nanosheets; (b) TEM image showing the cross section and thickness of a nanosheet; (c) HRTEM image taken from a flat face of nanosheet; (d) HRTEM image taken from a cross section of nanosheet.

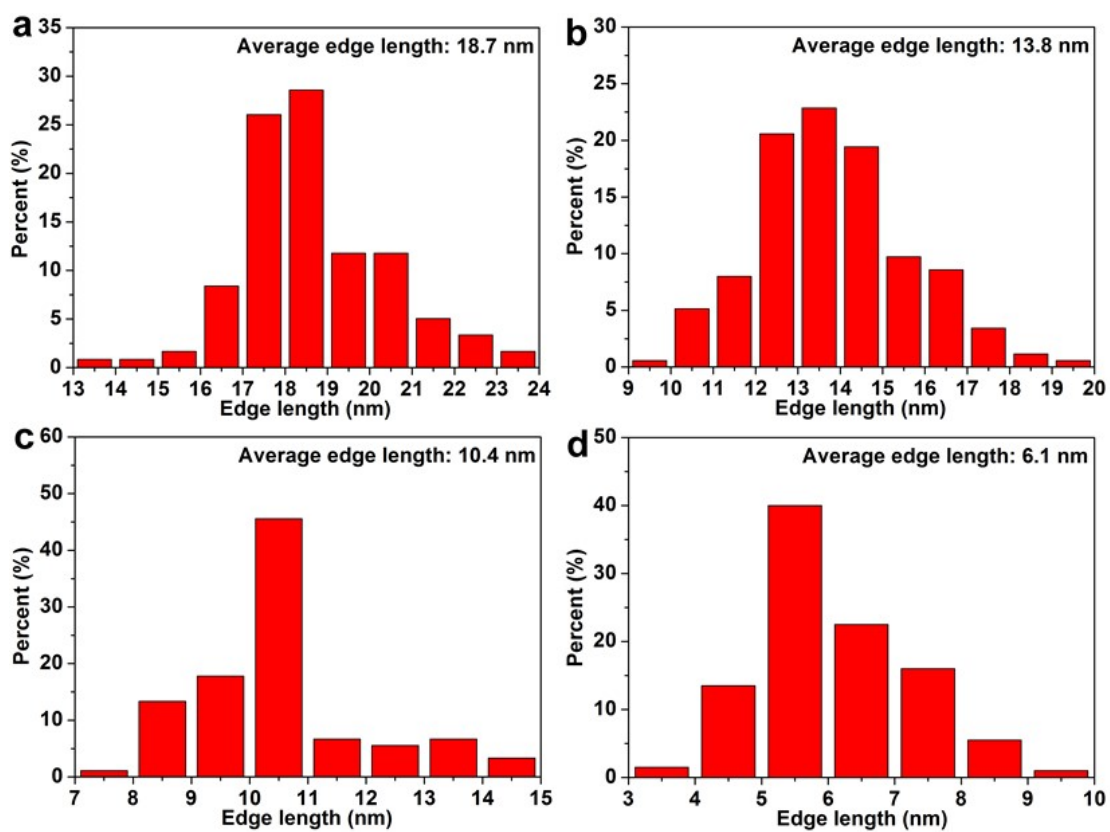


Fig. S2 Average edge length of Pd nanocubes in (a) $\text{TiO}_2\text{-Pd}_{\text{cub}-19}$, (b) $\text{TiO}_2\text{-Pd}_{\text{cub}-14}$, (c) $\text{TiO}_2\text{-Pd}_{\text{cub}-10}$ and (d) $\text{TiO}_2\text{-Pd}_{\text{cub}-6}$.

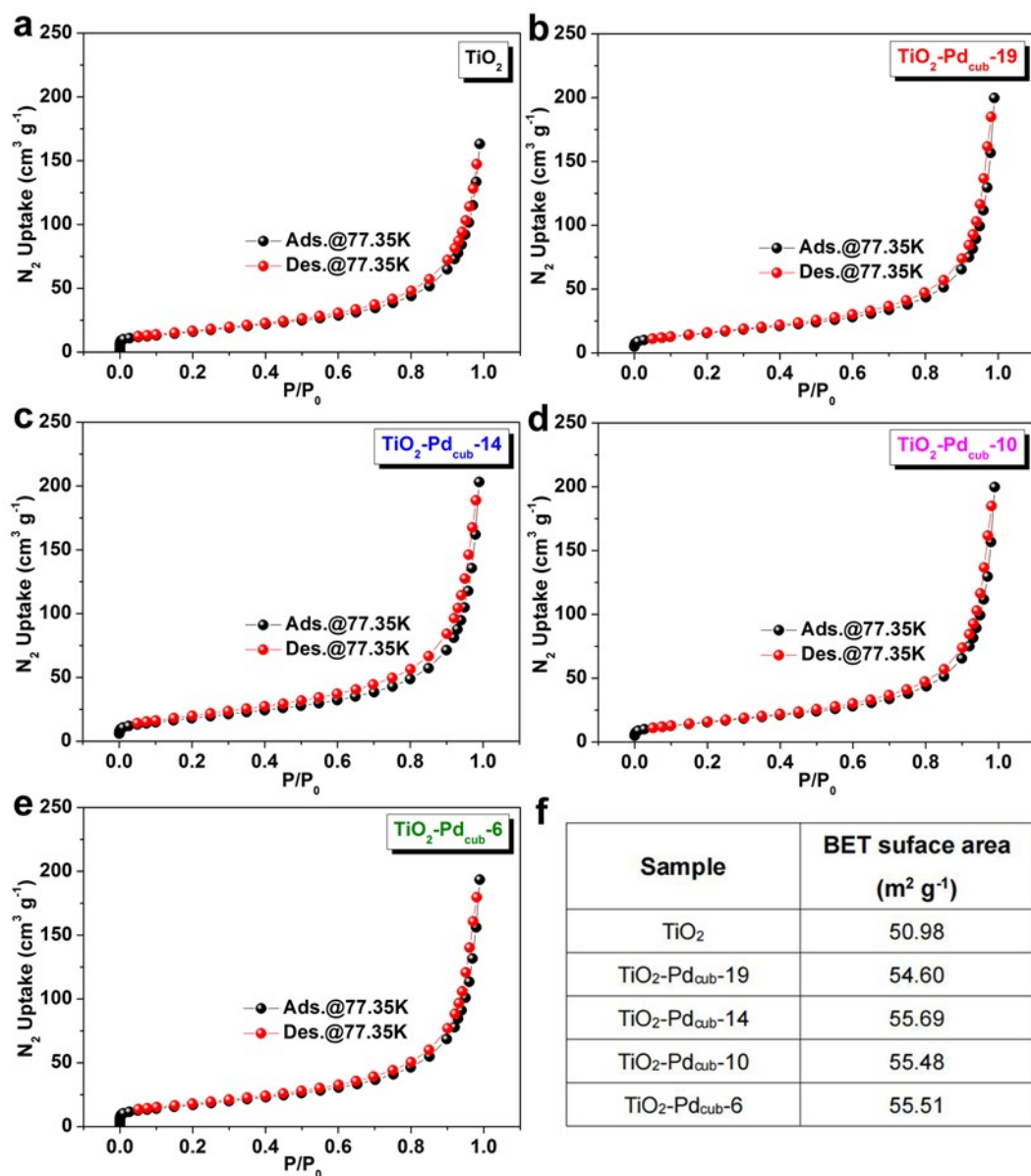


Fig. S3 Nitrogen adsorption- desorption isotherms for (a) TiO₂, (b) TiO₂-Pd_{cub}-19, (c) TiO₂-Pd_{cub}-14, (d) TiO₂-Pd_{cub}-10 and (e) TiO₂-Pd_{cub}-6 at 77.35 K, respectively. (f) calculated BET surface area of the samples.

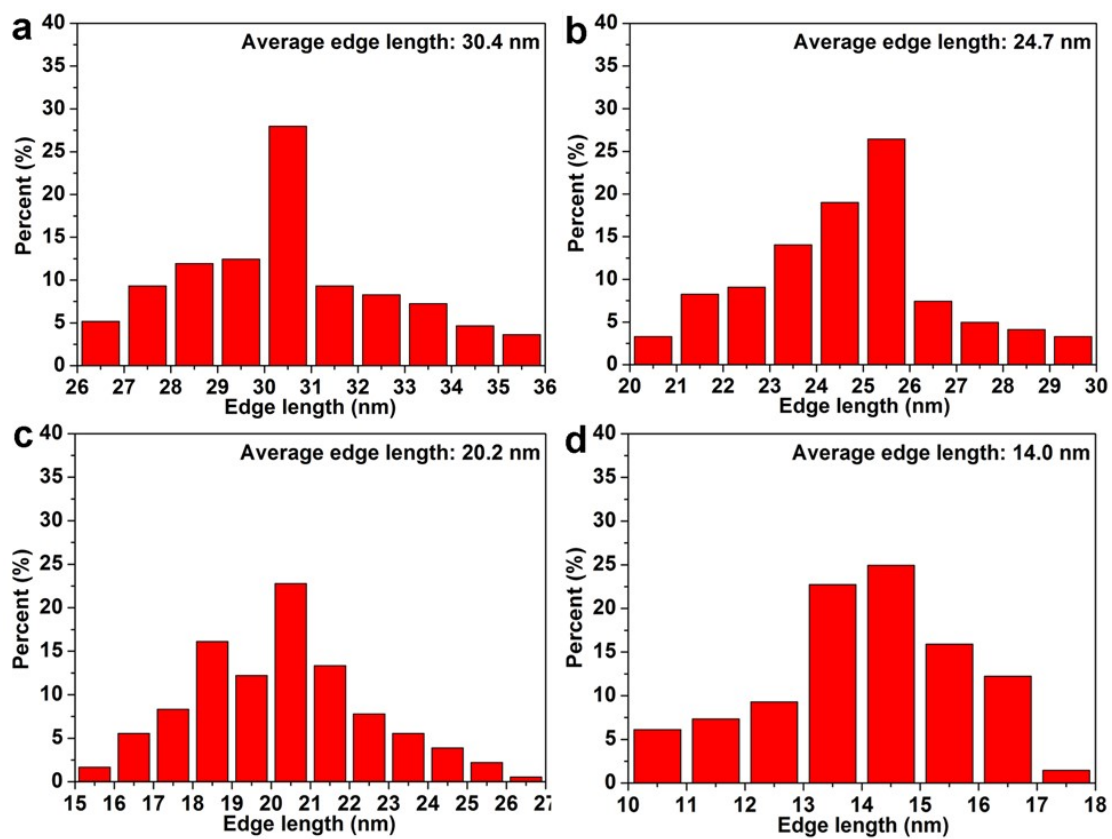


Fig. S4 Average edge length of Pd nanotetrahedrons in (a) $\text{TiO}_2\text{-Pd}_{\text{tet-30}}$, (b) $\text{TiO}_2\text{-Pd}_{\text{tet-25}}$, (c) $\text{TiO}_2\text{-Pd}_{\text{tet-20}}$ and (d) $\text{TiO}_2\text{-Pd}_{\text{tet-14}}$.

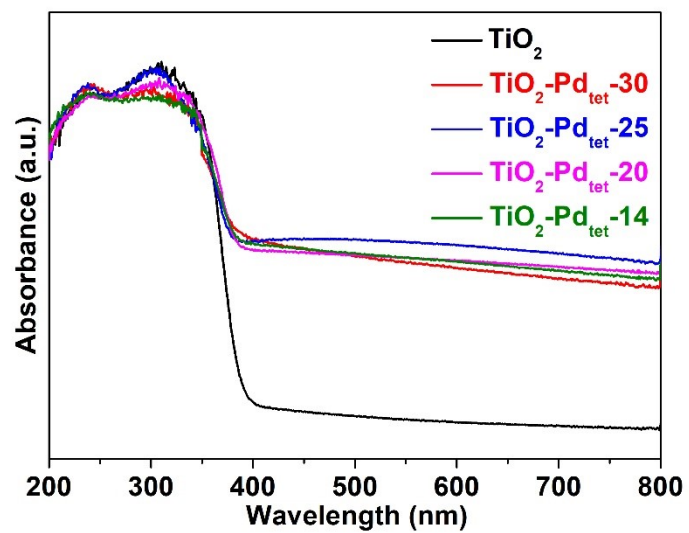


Fig. S5 UV-vis diffuse reflectance spectra of $\text{TiO}_2\text{-Pd}_{\text{tet}}$ samples with blank TiO_2 as a reference.

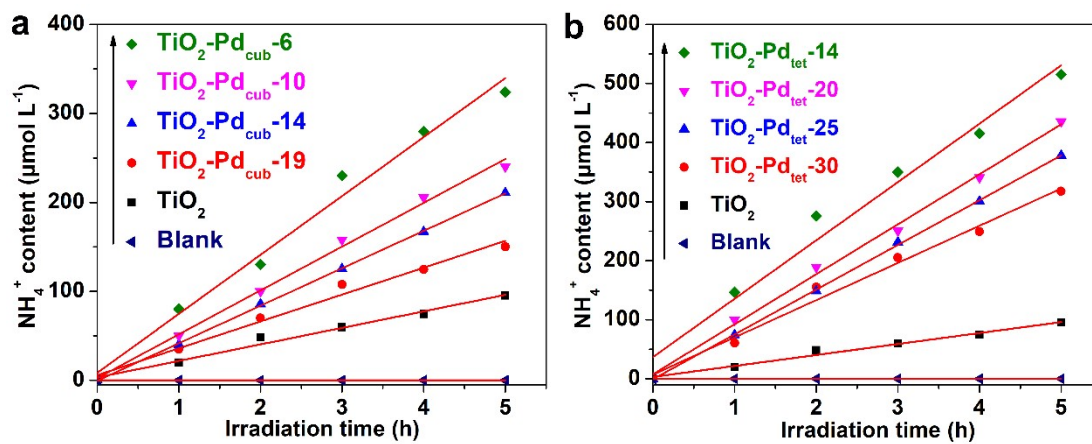


Fig. S6 Time course of photocatalytic N₂ fixation under UV light irradiation with (a) TiO₂-Pd_{cub} and (b) TiO₂-Pd_{tet} samples as catalysts.

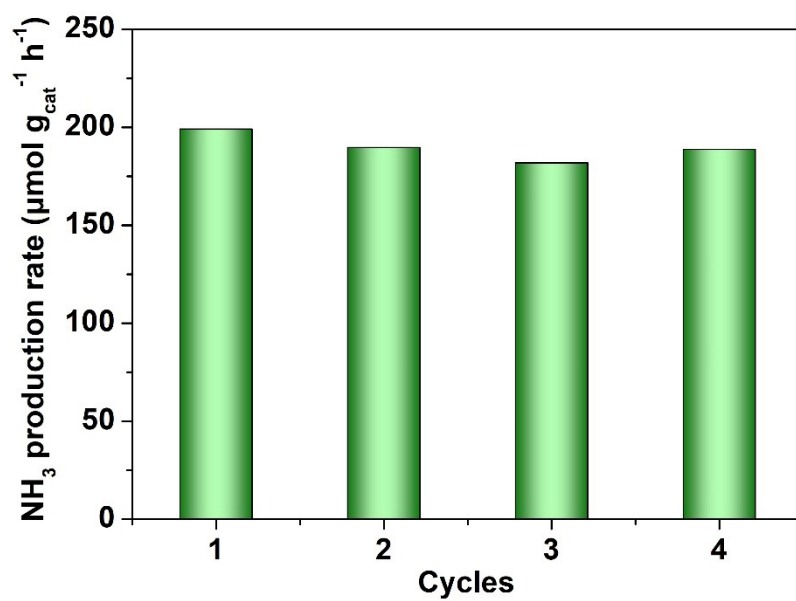


Fig. S7 Cycling tests of photocatalytic NH_3 production over $\text{TiO}_2\text{-Pd}_{\text{tet}}\text{-14}$.

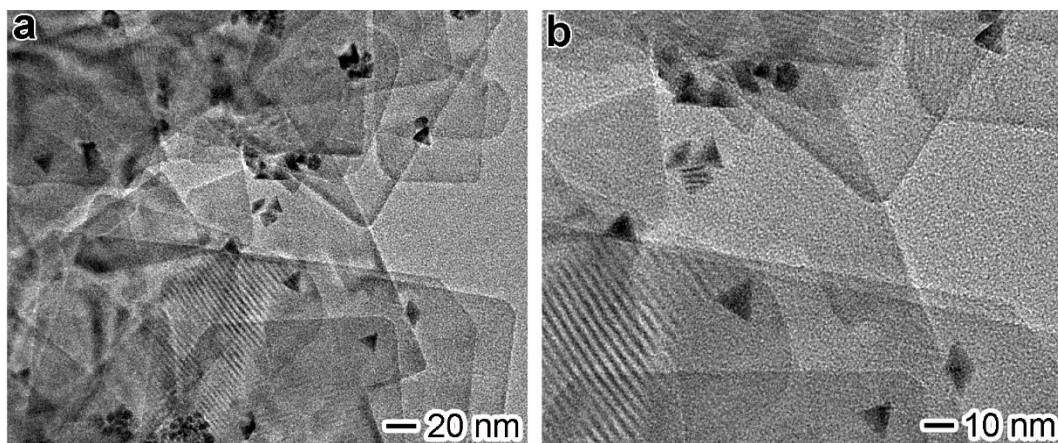


Fig. S8 TEM images of TiO₂-Pd_{tet}-14 after the photocatalytic cycles.

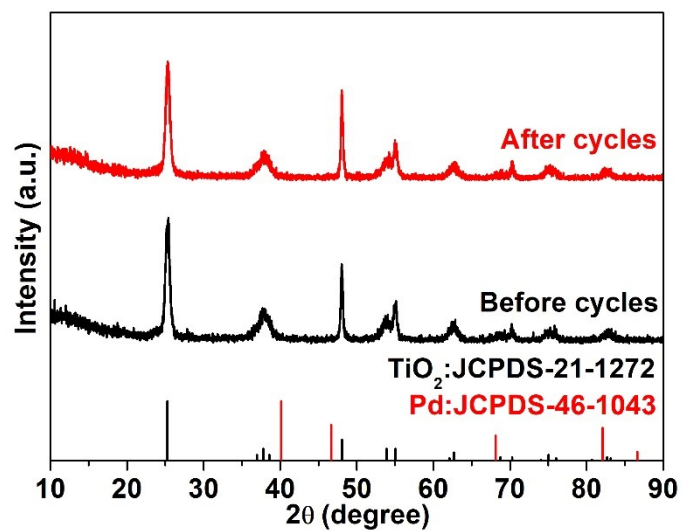


Fig. S9 XRD patterns of TiO₂-Pd_{tet}-14 before and after the photocatalytic cycles.

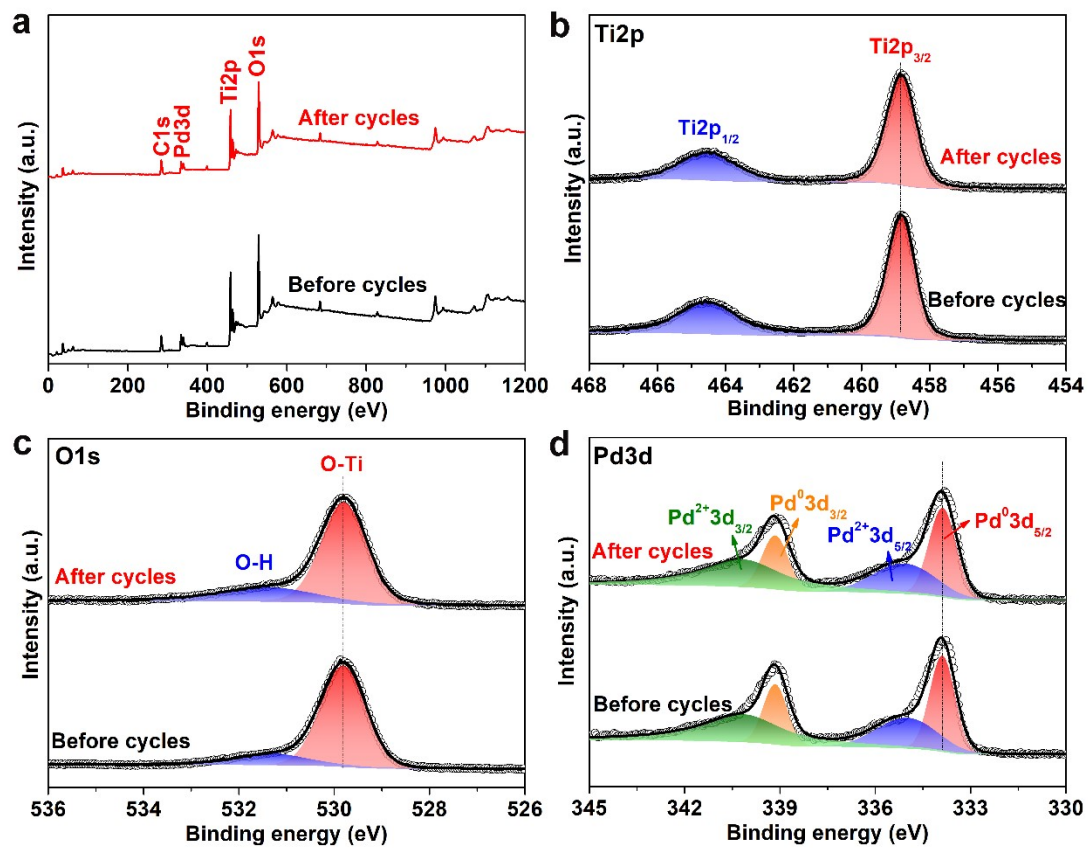


Fig. S10 XPS spectra of $\text{TiO}_2\text{-Pd}_{\text{tet}}\text{-14}$ before and after the photocatalytic cycles: (a) survey spectra, (b) Ti2p, (c) O1s and (d) Pd3d.

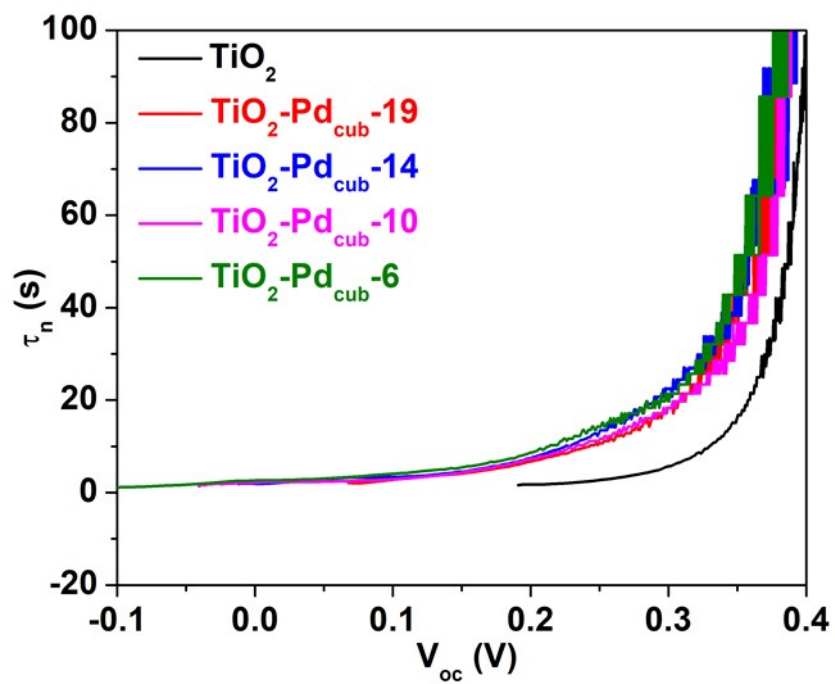


Fig. S11 Average lifetimes of the photo-generated charge carriers obtained from transient OCVD measurements.

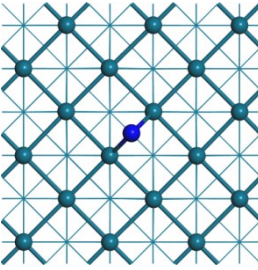
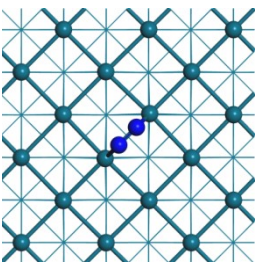
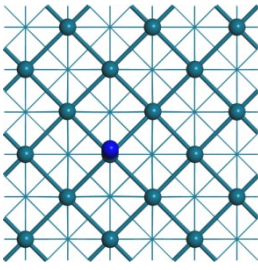
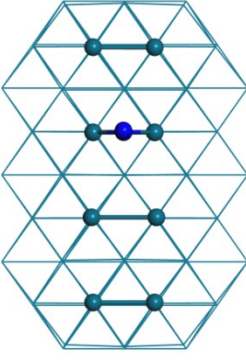
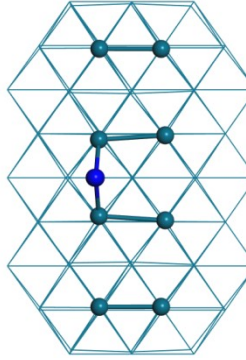
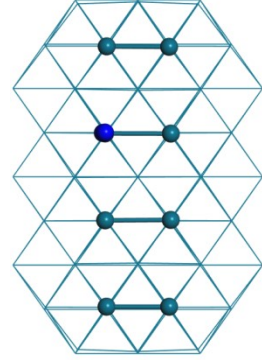
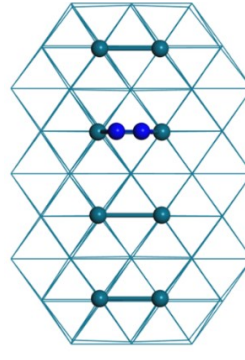
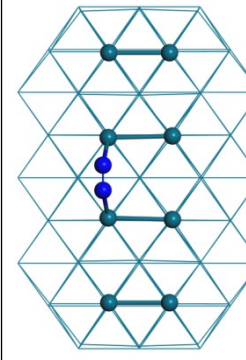
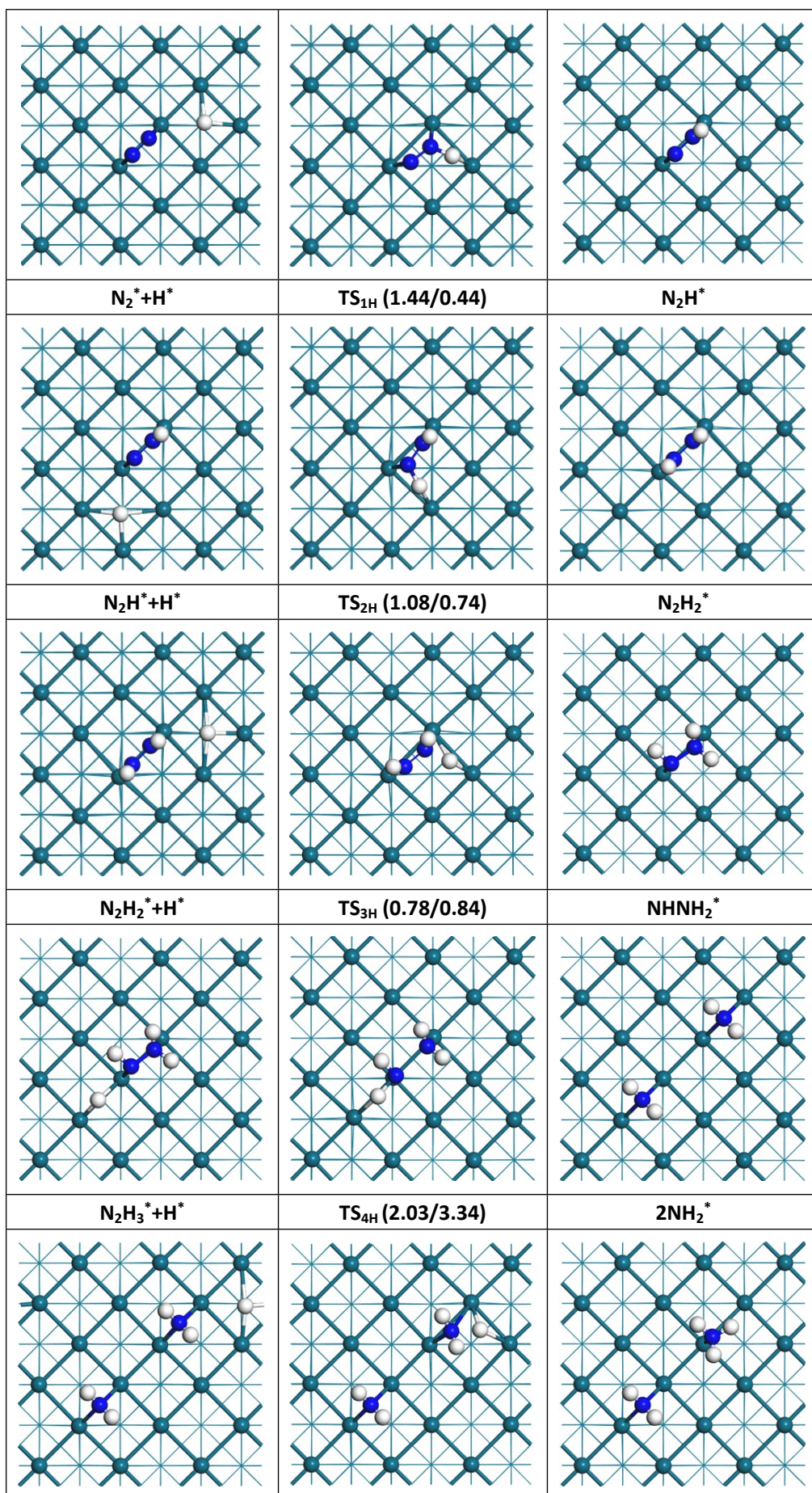
Surface				
				
$E_{\text{abs}} = -0.19$	$E_{\text{abs}} = -0.20$	$E_{\text{abs}} = -0.27$		
Edge				
				
$E_{\text{abs}} = -0.26$	$E_{\text{abs}} = -0.18$	$E_{\text{abs}} = -0.59$	$E_{\text{abs}} = -0.55$	$E_{\text{abs}} = -0.72$

Fig. S12 N₂ adsorption configurations and adsorption energies (eV) on surface and edge of Pd nanocubes.



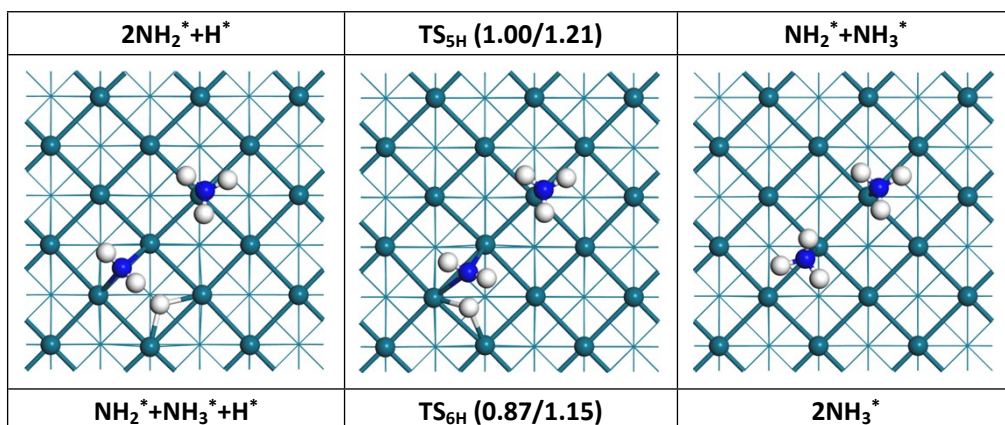
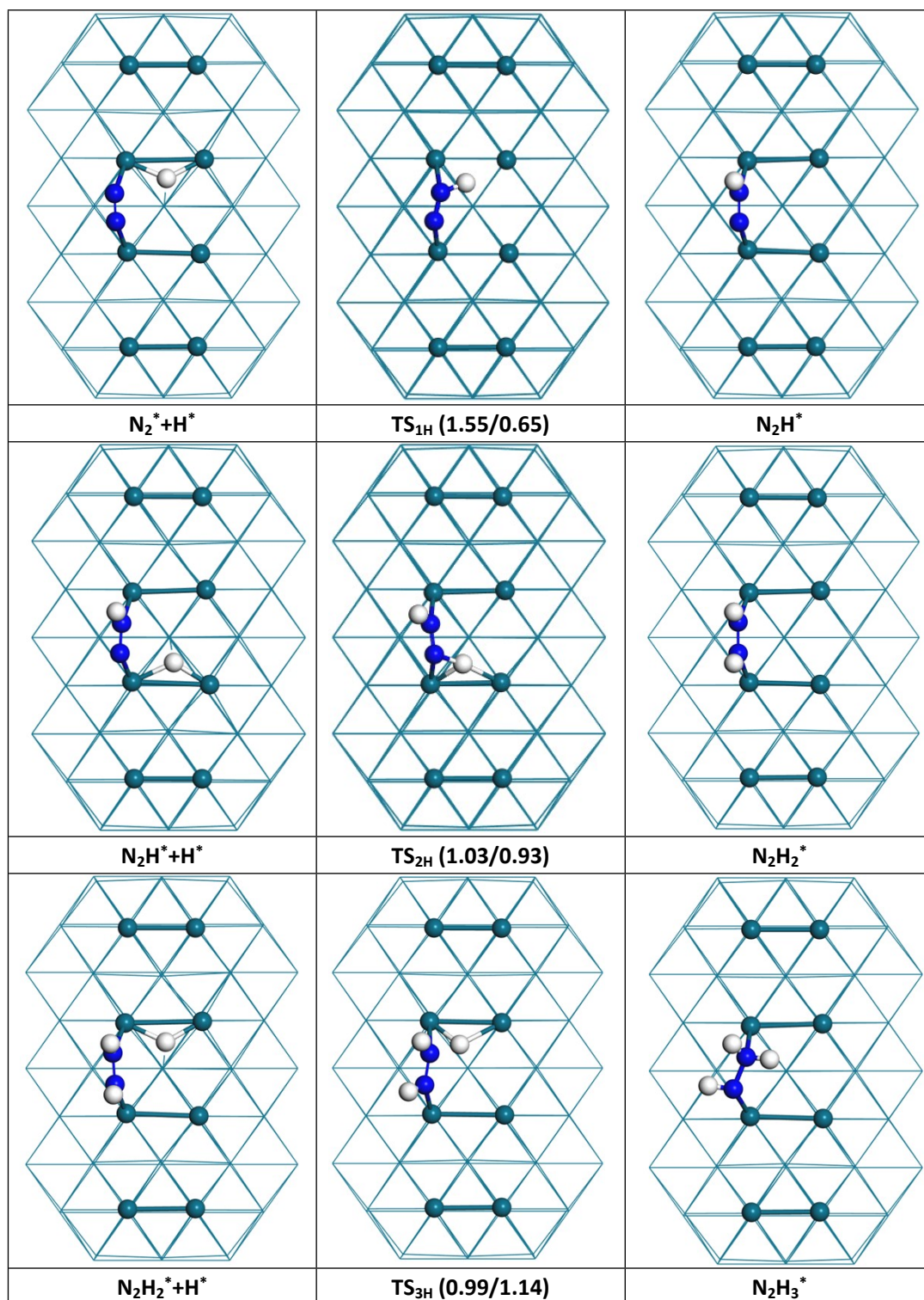


Fig. S13 N_2 hydrogenation on (100) surface of Pd nanocubes.



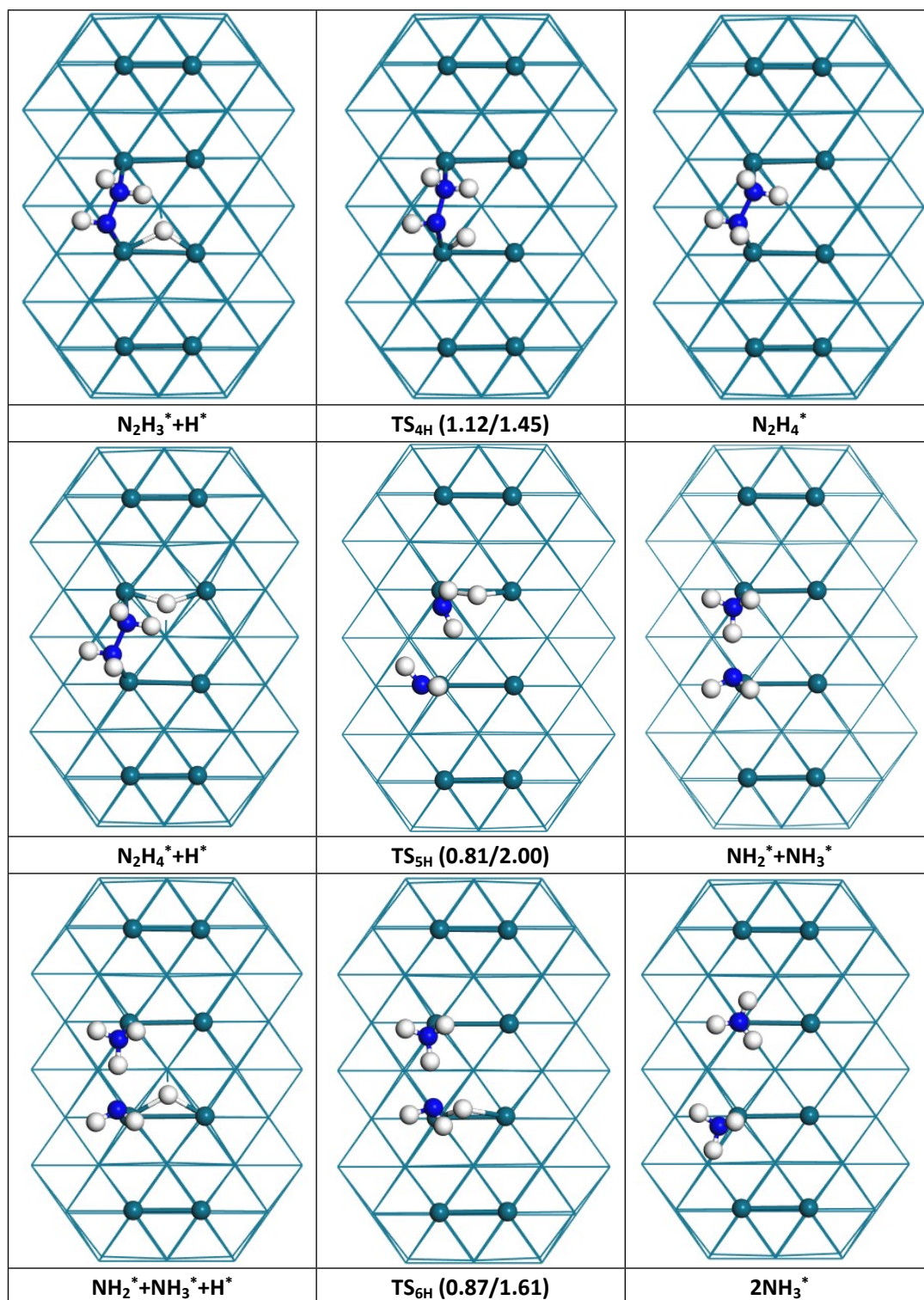


Fig. S14 N_2 hydrogenation at the edge of Pd nanocubes.

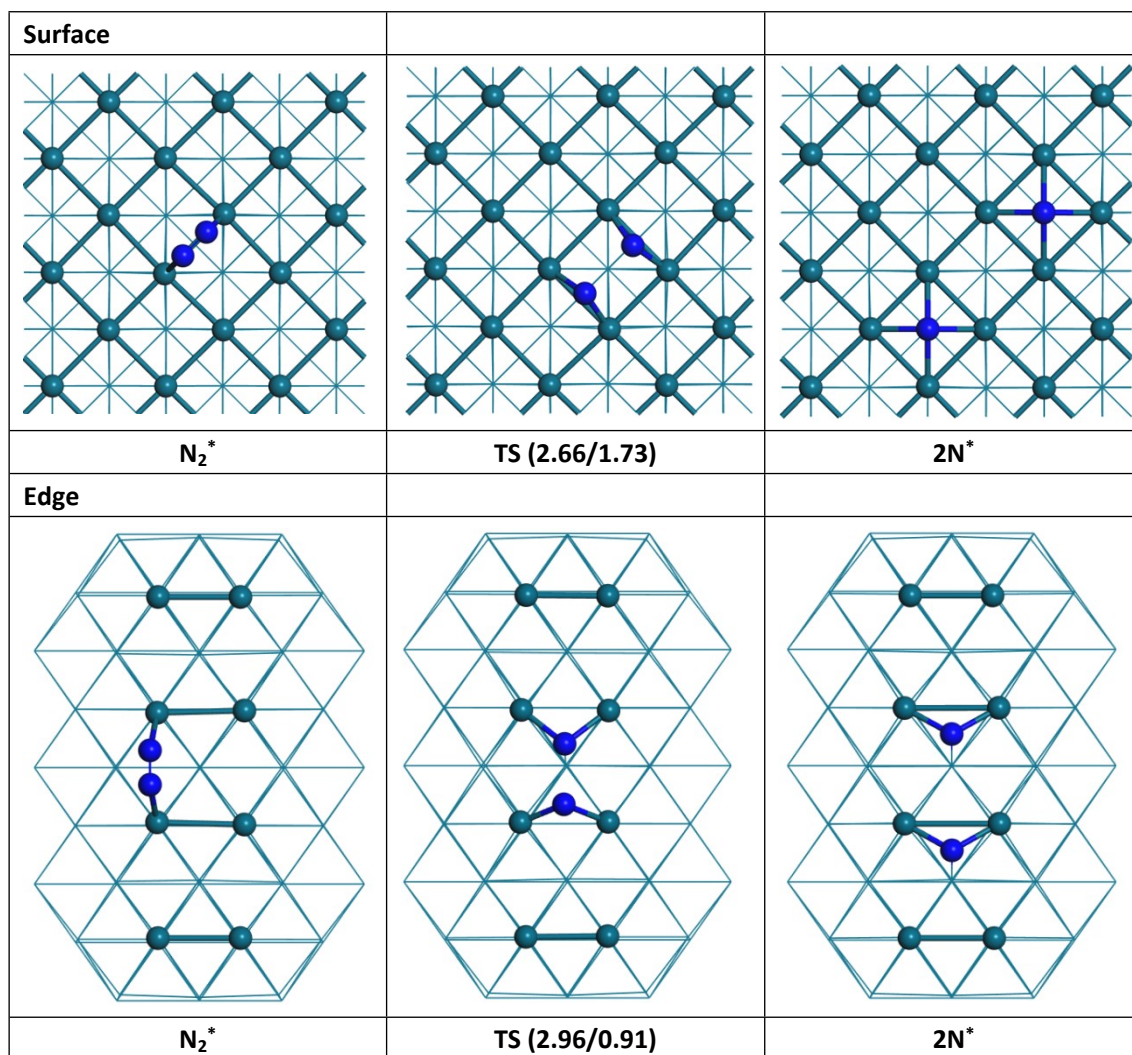
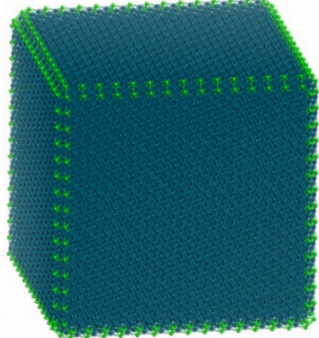


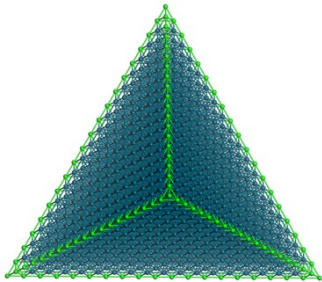
Fig. S15 N₂ dissociation on the surface and edge of Pd nanocubes.

Table S1. Calculation of the number of atoms in Pd nanocubes in different sizes according to the left model.

	Average sizes of Pd nanocubes (nm)	18.7	13.8	10.4	6.1
	Number of atoms on the edge (C5+C6)	1116	828	588	348
	Number of atoms on the surface (C8)	20230	11560	5760	1960
	$(C5+C6)/(C8)$	0.055	0.072	0.102	0.178
	$(C5+C6)/(C5+C6+C8)$	0.052	0.067	0.093	0.151
	Total number of atoms	441800	186200	70000	16200
	Ratio of surface atoms to total atoms (%)	4.6	6.2	8.2	12.1
	Loading amounts of Pd (wt.%)	9.1	6.7	5.0	3.0

C5, C6, C8 indicate that the atomic coordination number is 5, 6, 8, respectively. C5 and C6 are shown in green. C8 is shown in dark blue. Note that only 5 facets of Pd nanocube were involved due to the contact of one (100) surface with TiO₂.

Table S2. Calculation of the number of atoms in Pd nanotetrahedrons in different sizes according to the left model.

	Average sizes of Pd nanotetrahedrons (nm)	30.4	24.7	20.2	14.0
	Number of atoms on the edge (C3+C6)	652	532	436	298
	Number of atoms on the surface (C9)	17334	11484	7668	3528
	$(C3+C6)/(C9)$	0.038	0.046	0.057	0.084
	$(C3+C6)/(C3+C6+C9)$	0.036	0.044	0.054	0.078
	Total number of atoms	227920	125580	70300	23426
	Ratio of surface atoms to total atoms (%)	7.6	9.1	10.9	15.1
	Loading amounts of Pd (wt.%)	5.0	4.3	3.4	2.4

C3, C6, C9 indicate that the atomic coordination number is 3, 6, 9, respectively. C3 and C6 are shown in green. C9 is shown in dark blue. Note that only 3 facets of Pd nanotetrahedron were involved due to the contact of one (111) surface with TiO₂.

References

- S1 X. Han, Q. Kuang, M. Jin, Z. Xie and L. Zheng, *J. Am. Chem. Soc.*, 2009, **131**, 3152-3153.